Facile synthesis of Ag_3PO_4 microcrystals and its enhanced photocatalytic disinfection

Chi-Shun Tseng[1], *Tsunghsueh Wu*[2], *Yang-Wei Lin*[1] ✉

[1]*Department of Chemistry, National Changhua University of Education, Changhua City 500, Taiwan*
[2]*Department of Chemistry, University of Wisconsin-Platteville, 1 University Plaza, Platteville, WI 53818-3099, USA*
✉ *E-mail: linywjerry@cc.ncue.edu.tw*

Published in Micro & Nano Letters; Received on 14th April 2018; Revised on 25th May 2018; Accepted on 11th July 2018

Facile synthesis of silver phosphate (Ag_3PO_4) microcrystals was developed for the novel application in the disinfection of pathogens with visible light. Ag_3PO_4 microcrystals from different synthesis routes were produced and characterised by scanning electron microscopy and UV–visible diffuse reflectance spectroscopy. The antibacterial activity of the Ag_3PO_4 microcrystals was also evaluated for its effectiveness in eradicating pathogens (*Escherichia coli* and *Staphylococcus aureus*) under white-light light-emitting-diode irradiation. The prepared Ag_3PO_4 microcrystals displayed higher and more stable photocatalytic antibacterial activity (>99% eradication rate within 10 min) comparing to Ag^+ ions used only. This can be attributed to the oxidation of the photogenerated hole and the adsorption of Ag^+ ions. This study demonstrated the strong photocatalytic activity of the as-prepared Ag_3PO_4 microcrystals, promising for industrial applications related to the eradication of pathogens from wastewater.

1. Introduction: Water pollution caused by pathogens posts a serious threat to public health and combating this issue has been progressed [1–4]. Traditionally, pathogens in water are eliminated by chlorination, ozonation, and UV irradiation [5]. Although they are the existing means to treat wastewater, they involve with the use of hazardous chemicals and high energy input. In recent years, a concept of using semiconductor-based photocatalysts with the capability of degrading organic dyestuffs and eradicating pathogens under light irradiation has been developed [4, 6]. A heterogeneous photocatalyst, TiO_2, is considered attractively because it is widely used, low cost, non-toxicity, and high stability. However, its inherited rapid electron–hole recombination rate hinders its effectiveness in wastewater treatment in addition to other issues such as its photo-instability and limited antimicrobial ability [7]. Furthermore, TiO_2 has a wide bandgap of 3.2 eV, which indicates its photocatalytic activity can only be activated by UV light and is expected to perform inefficiently in sunlight [8]. Thus, development of a stable visible-light-responsive photocatalyst will make an important impact in removing pathogens in wastewater. In 2010, Ag_3PO_4 was synthesised to demonstrate high photocatalytic activity for O_2 generation from water and good photodegradation of organic dyes under visible light [9]. Their study showed ten folds of improvement in the photodegradation rate of organic dyes by Ag_3PO_4 over other visible-light-responsive photocatalysts such as $BiVO_4$ and N-doped TiO_2. Following this discovery, many studies have been carried out on the synthesis of Ag_3PO_4 photocatalysts with different morphology and their photocatalytic activity [10–19]. Among the studies conducted on Ag_3PO_4, those investigating the photocatalytic disinfection mechanism of Ag_3PO_4 are rare.

Herein, Ag_3PO_4 microcrystals were produced by a sonochemical procedure (20 kHz, 600 W for 30 min) with or without a hydrothermal condition (180°C for 24 h) and their photocatalytic activity was examined. The photocatalytic antibacterial activity of the as-prepared Ag_3PO_4 microcrystals was assessed according to their ability to disinfect *Escherichia coli* (*E. coli*) and *Staphylococcus aureus* (*S. aureus*) under low-power white-light light-emitting-diode (LED) irradiation (5 W). Finally, the possible photocatalytic mechanisms of pathogen disinfection using the Ag_3PO_4 microcrystals were also examined.

2. Experimental

2.1. Preparation: All reagents used were of analytical grade and without further purification. Ag_3PO_4 microcrystals (S0) were prepared using a sonochemical method alone. The typical preparation was as follows: Two solutions, 0.28 mM of $AgNO_3$ (45 ml) and 0.84 mM of Na_3PO_4 (5 ml), were sonicated in a beaker at room temperature by immersing a high-frequency ultrasonic probe (Misonix, Inc., Farmingdale, NY, USA: XL-2020, 20 kHz, 600 W) directly in the solution. After 30 min of sonification, the precipitates were filtered and washed three times with deionised water and ethanol before they were dried in a desiccator at 50°C for 8 h. Ag_3PO_4 microcrystals (S1) were prepared with a combination of a sonochemical and hydrothermal method. $AgNO_3$ (0.28 mM) was dissolved in 45 ml of deionised water. The Na_3PO_4 solution (0.84 mM, 5 ml) was then added to the preceding solution under sonification at room temperature. After 30 min of sonication, the resulting mixture was transferred to a 50 ml Teflon-lined stainless steel autoclave. Hydrothermal synthesis was performed at 180°C for 24 h in an electric oven. The reaction mixture was allowed to cool at 25°C. The precipitates were filtered and washed with deionised water and ethanol for three times before they were dried in a desiccator at 50°C for 8 h.

2.2. Characterisation: A HITACHI S-4800 scanning electron microscope (SEM) (Hitachi High-Technologies Corporation, Tokyo, Japan) operating at 15 kV was used to observe the morphologies of the Ag_3PO_4 microcrystals. A SMART APEX II X-ray diffractometer (Bruker AXS, Billerica, MA, USA) with Cu Kα radiation ($\lambda = 0.15418$ nm) was used to determine the crystalline phases of the Ag_3PO_4 microcrystals. An Evolution 2000 UV–Vis spectrometer (Thermo Fisher Scientific Inc., Madison, WI, USA) with $BaSO_4$ bulk material as the reference material was used to find the UV–visible diffuse reflectance spectra (UV–vis-DRS) of the Ag_3PO_4 microcrystals.

2.3. Photocatalytic antibacterial activity: *E. coli* (*CV514*) and *S. aureus* (*wild*) were used as gram-negative and gram-positive bacterial modes, respectively, in the evaluation of the antibacterial activity of the Ag_3PO_4 microcrystals (S0 and S1) based on a previously described procedure [20–22]. The microbes were cultured at 37°C in a Luria–Bertani (LB) medium. The microbes were then separated and washed by centrifugation and finally, they were re-suspended in the LB medium with a concentration of 10^6 cfu/ml. In each antibacterial test, 50 ml of bacterial suspension was added to 5 mg of solid Ag_3PO_4 microcrystals and the mixture was kept under a low-power white-light LED

doi: 10.1049/mnl.2018.5049

irradiation (5 W) or in the dark with a continuous stirring. For evaluation, the disinfection efficiency, 100 µl of the suspension was removed at fixed time intervals, then diluted to 10^3cfu/ml with the LB medium and incubated at 37°C for 24 h. The number of cells was determined by counting the colonies formed on the plate. At the end of each experiment, the concentration of silver ions in the solution was determined using the atomic absorption spectrophotometer (GBC scientific equipment, Braeside, VIC, Australia).

2.4. Scavenger test: The procedure for counting photo-generated holes was similar to that adopted in the photocatalytic antibacterial activity experiment [20–24]. Hole scavengers (EDTA, 10.0 µM) were added to the bacterial solution prior to the addition of the Ag_3PO_4 microcrystals.

3. Results and discussion: Fig. 1 shows the SEM images of the Ag_3PO_4 microcrystals from two different synthetic routes and they reveal notable differences in the morphology and size of particles. The Ag_3PO_4 microcrystals (S0) appear as small quasi-spherical-like structures (Fig. 1*a*). During the Ag_3PO_4 sample (S0) preparation, the solution turns turbid after 5 min of sonication. No diffraction peaks were observed from XRD analysis, suggesting the amorphous nature of Ag_3PO_4 microcrystals produced from a brief sonication. After an extended sonication to 25 min, yellow precipitates began to form. These results strongly suggest the crystallisation of amorphous Ag_3PO_4 samples. Fig. 1*b* shows that the main diffraction peaks for the prepared Ag_3PO_4 microcrystals (S0) can be primarily indexed to a body-centred cubic structure (JCPDS Card No. 06-0505). As the time of sonication is extended and the concentration of particles increases, more particles can collide with sufficient energy provided by sonication and aggregate into bigger particles. In addition, the mass transport in turbulent mixing can be improved by sonication, leading to the formation of the final products with quasi-spherical-like morphology [23]. For Ag_3PO_4 microcrystals (S1) produced by the combination of 30 min sonication and a subsequent hydrothermal treatment, the further growth is found. The hydrothermal process provided energy for the Ag_3PO_4 to produce large crystalline microcrystals with quasi-spherical-like shape [23]. Therefore, the Ag_3PO_4 microcrystals (S1) were composed of quasi-spherical-like structures with a diameter of 4.5 ± 1.7 µm (Fig. 1*b*). According to the main diffraction peaks (Fig. 1*d*) and Joint Committee on Powder Diffraction Standards 06-0505, the crystalline phase of the prepared Ag_3PO_4 (S1) is also a body-centred cubic structure, indicating that the hydrothermal procedure has no influence on the crystalline phase of the Ag_3PO_4 microcrystals. The UV–vis-DRS spectra of the Ag_3PO_4 microcrystals shown in Fig. 2 reveal that the yellow Ag_3PO_4 microcrystals absorbed both UV and a major part of visible light. The data also show a linear correlation between the square root of the absorption coefficient ($(\alpha hv)^{0.5}$) and incident photon energy (hv), which strongly suggests the absorption edges of all the Ag_3PO_4 microcrystals were due to indirect transitions (inset in Fig. 2). The corresponding energy bandgaps (E_g) of the Ag_3PO_4 microcrystals were determined from the x-axis intercept of the curve tangent in the plot of $(\alpha hv)^{0.5}$ versus hv (inset in Fig. 2) [22, 25]. The estimated bandgaps for S0 and S1 microcrystals were 2.41 and 2.36 eV, respectively.

The photocatalytic antibacterial activity of S0, S1 and Ag^+ ions toward was evaluated under the light and dark conditions. In the absence of the Ag_3PO_4 microcrystals and Ag^+ ions, the count of both bacterial strains did not change under both conditions as shown by the black curve in Fig. 3. The red and green curves in Figs. 3*a* and *c* reveal the antibacterial activity of S0 and S1 in the dark and within 15 min they reduced the amount of *E. coli* by 97.9 and 64.8%, respectively. It is well-known that the antibacterial activity of Ag nanoparticles is caused by the release of Ag^+ [26, 27]. The results presented in Fig. 3 (blue curve) prove that Ag^+ ions (0.075 mM) possessed antibacterial activity toward *E. coli* and *S. aureus* and encouragingly S0 and S1 are found exceeding the performance of Ag^+ ions in disinfection under the white light irradiation. Because S0 with a low degree of crystallinity, it is facile to release Ag^+ ions from the Ag_3PO_4 microcrystals into the LB medium [20]. Therefore, compared to S1 (*E. coli*: 0.055 mM, *S. aureus*: 0.048 mM), the concentration of Ag^+ ions released from S0 (*E. coli*: 0.073 mM, *S. aureus*: 0.077 mM) are higher, promoting the intrinsic antibacterial activity of S0.

Compared with the dark condition, S0 showed no improvement in the disinfection activity under white-light LED irradiation (red curve in Figs. 3*b* and *d*). This may be because Ag^+ ions are the major species involved in the eradication of bacteria for S0 through solubility product equilibrium. The green curve in Figs. 3*b* and *d* indicates the photocatalytic antibacterial activity of S1 under white-light LED irradiation. In the presence of S1, >99% of both bacterial strains was eradicated within 10 min. Thus, S1 exhibited excellent light-enhanced disinfection ability. This may be because photogenerated holes are reactive with bacterial membranes and cause significant damage to bacteria [26]. The photocatalytic induced damage to the bacterial membranes enhanced the intake of Ag^+ to live bacteria and, as a result, inhibited

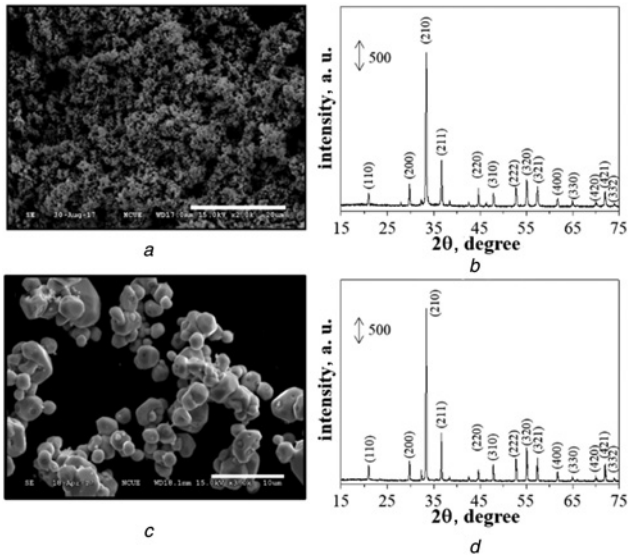

Fig. 1 *SEM images and XRD spectra of Ag_3PO_4 synthesised under sonochemical process (600 W) at 25 kHz for 30 min*
a, *b* Without and
c, *d* With the hydrothermal process at 180°C for 24 h. Scale bar: (a) 20 µm and (c) 10 µm

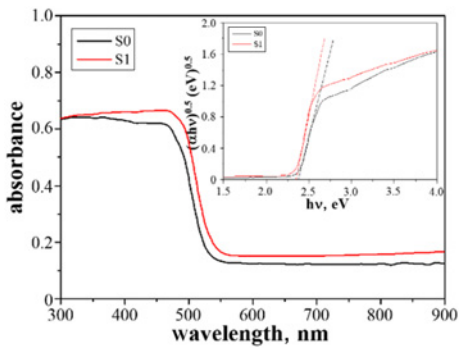

Fig. 2 *UV–vis-DRS spectra of S0 and S1. Inset: $(\alpha hv)^{0.5}$ versus hv of the corresponding microcrystals*

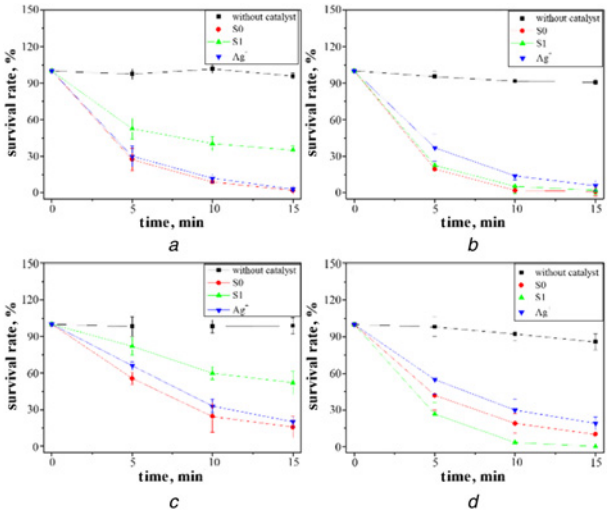

Fig. 3 *Survival rate (%) of E. coli*
a In the dark and
b Under white-light LED irradiation without and with microcrystals (S0, S1 and Ag^+ ions); *S. aureus*
c In the dark and
d Under white-light LED irradiation without and with microcrystals (S0, S1 and Ag^+ ions). Each data point and error bar represent the mean and standard deviation ($n = 3$), respectively

enzyme functions and led to the death of bacteria. The residual concentration of Ag^+ ions after photolysis was measured through atomic absorption spectroscopy. When S1 was used, the concentration of Ag^+ was 90.1 and 85.6% lower after application to *E. coli* and *S. aureus*, respectively, much larger decrease than the results when only Ag^+ was used (*E. coli*: 38.7%, *S. aureus*: 24.1%). Furthermore, a hole-scavenger test was performed. In the presence of the hole scavenger, the photocatalytic antibacterial activity of S1 under white-light LED irradiation decreased to 61.9 and 77.5% for *E. coli* and *S. aureus*, respectively. Therefore, S1 possesses light-enhanced disinfection activity. On the basis of these results, the photocatalytic disinfection mechanism of the Ag_3PO_4 microcrystals (S1) is presented. Photogenerated holes are reactive and nonselective oxidants that can damage bacterial membranes effectively. Because of the initial damage to bacterial membranes, numerous Ag^+ released from Ag_3PO_4 microcrystals are able to be absorbed by bacteria, inhibiting the bacteria's enzymatic functions and enhancing bacteria death.

4. Conclusion: Ag_3PO_4 microcrystals were synthesised using a combination of sonochemical and hydrothermal processes. Ag_3PO_4 microcrystals (S1) exhibited light-enhanced disinfection activity (>99% eradication of *E. coli* and *S. aureus* within 10 min) due to their ability to cause oxidative damage to the bacterial membrane from photogenerated holes and the absorption of Ag^+ under white-light LED irradiation. This study demonstrated the potential of the Ag_3PO_4 microcrystals (S1) in a wide variety of industrial applications for the elimination of pathogens from wastewater.

5. Acknowledgments: This study was supported by the Ministry of Science and Technology under contract (MOST 106-2119-M-018-001). The authors thank Wallace Academic Editing for the English language editing.

6 References

[1] Ibrahim R.K., Hayyan M., AlSaadi M.A., *ET AL.*: 'Environmental application of nanotechnology: air, soil, and water', *Environ. Sci. Pollut. Res.*, 2016, **23**, pp. 13754–13788
[2] Wang P.H.: 'Membrane photoreactors (MPRS) for photocatalysts separation and pollutants removal: recent overview and new perspectives', *Sep. Sci. Technol.*, 2016, **51**, pp. 147–167
[3] Fernandez L. Esteves V.I., Cunha A., *ET AL.*: 'Photodegradation of organic pollutants in water by immobilized porphyrins and phthalocyanines', *J. Porphyr. Phthalocyanines*, 2016, **20**, pp. 150–166
[4] Lee K.M., Lai C.W., Ngai K.S., *ET AL.*: 'Recent developments of zinc oxide based photocatalyst in water treatment technology: a review', *Water Res.*, 2016, **88**, pp. 428–448
[5] Booshehri A.Y., Goh S.C.K., Hong J.D., *ET AL.*: 'Effect of depositing silver nanoparticles on $BiVO_4$ in enhancing visible light photocatalytic inactivation of bacteria in water', *J. Mater. Chem. A*, 2014, **2**, pp. 6209–6217
[6] Zainullina V.M., Zhukov V.P., Korotin M.A.: 'Influence of oxygen nonstoichiometry and doping with 2p-, 3p-, 6p- and 3d-elements on electronic structure, optical properties and photocatalytic activity of rutile and anatase: Ab initio approaches', *J. Photochem. Photobiol. C-Photochem. Rev.*, 2015, **22**, pp. 58–83
[7] Dong H.R., Zeng G.M., Tang L., *ET AL.*: 'An overview on limitations of TiO_2-based particles for photocatalytic degradation of organic pollutants and the corresponding countermeasures', *Water Res.*, 2015, **79**, pp. 128–146
[8] Kamalakkannan J., Chandraboss V.L., Prabha S., *ET AL.*: 'Preparation and characterization of $TiInVO_6$-nanomaterial using precipitation method and its multi applications', *J. Mater. Sci.-Mater. Electron.*, 2016, **27**, pp. 2488–2503
[9] Yi Z., Ye J., Kikugawa N., *ET AL.*: 'An orthophosphate semiconductor with photooxidation properties under visible-light irradiation', *Nat. Mater.*, 2010, **9**, pp. 559–564
[10] Yan X., Gao Q., Qin J., *ET AL.*: 'Morphology-controlled synthesis of Ag_3PO_4 microcubes with enhanced visible-light-driven photocatalytic activity', *Ceram. Int.*, 2013, **39**, pp. 9715–9720
[11] Yang Z.-M., Liu Y.-Y., Xu L., *ET AL.*: 'Facile shape-controllable synthesis of Ag_3PO_4 photocatalysts', *Mater. Lett.*, 2014, **133**, pp. 139–142
[12] Dong L., Wang P., Wang S., *ET AL.*: 'A simple way for Ag_3PO_4 tetrahedron and tetrapod microcrystals with high visible-light-responsive activity', *Mater. Lett.*, 2014, **134**, pp. 158–161
[13] Hao Z., Ai L., Zhang C., *ET AL.*: 'Self-sacrificial synthesis of porous Ag_3PO_4 architectures with enhanced photocatalytic activity', *Mater. Lett.*, 2015, **143**, pp. 51–54
[14] Dong P., Yin Y., Xu N., *ET AL.*: 'Facile synthesis of tetrahedral Ag_3PO_4 mesocrystals and its enhanced photocatalytic activity', *Mater. Res. Bull.*, 2014, **60**, pp. 682–689
[15] Wan J., Sun L., Fan J., *ET AL.*: 'Facile synthesis of porous Ag_3PO_4 nanotubes for enhanced photocatalytic activity under visible light', *Appl. Surf. Sci.*, 2015, **355**, pp. 615–622
[16] Guo X., Chen C., Yin S., *ET AL.*: 'Controlled synthesis and photocatalytic properties of Ag_3PO_4 microcrystals', *J. Alloy. Compd.*, 2015, **619**, pp. 293–297
[17] Li J., Ji X., Li X., *ET AL.*: 'Preparation and photocatalytic degradation performance of Ag_3PO_4 with a two-step approach', *Appl. Surf. Sci.*, 2016, **372**, pp. 30–35
[18] Xie Y., Huang Z., Zhang Z., *ET AL.*: 'Controlled synthesis and photocatalytic properties of rhombic dodecahedral Ag_3PO_4 with high surface energy', *Appl. Surf. Sci.*, 2016, **389**, pp. 56–66
[19] Frontistis Z., Antonopoulou M., Petala A., *ET AL.*: 'Photodegradation of ethyl paraben using simulated solar radiation and Ag_3PO_4 photocatalyst', *J. Hazard. Mater.*, 2017, **323**, pp. 478–488
[20] Chen Y.-J., Tseng C.-S., Tseng P.-J., *ET AL.*: 'Synthesis and characterization of Ag/Ag_3PO_4 nanomaterial modified $BiPO_4$ photocatalyst by sonochemical method and its photocatalytic application', *J. Mater. Sci.-Mater. Electron.*, 2017, **28**, pp. 11886–11899
[21] Huang C.-K., Wu T., Huang C.-W., *ET AL.*: 'Enhanced photocatalytic performance of $BiVO_4$ in aqueous $AgNO_3$ solution under visible light irradiation', *Appl. Surf. Sci.*, 2017, **399**, pp. 10–19
[22] Huang T.-Y., Chen Y.-J., Lai C.-Y., *ET AL.*: 'Synthesis, characterization, enhanced sunlight photocatalytic properties, and stability of Ag/Ag_3PO_4 nanostructure-sensitized $BiPO_4$', *RSC Adv.*, 2015, **5**, pp. 43854–43862
[23] Cheng L.-W., Tsai J.-C., Huang T.-Y., *ET AL.*: 'Controlled synthesis, characterization and photocatalytic activity of $BiPO_4$ nanostructures with different morphologies', *Mater. Res. Express*, 2014, **1**, pp. 1–19, doi: 10.1088/2053-1591/1/2/025023
[24] Huang C.-W., Wu M.-Y., Lin Y.-W.: 'Solvothermal synthesis of Ag hybrid $BiPO_4$ heterostructures with enhanced photodegradation activity and stability', *J. Colloid Interf. Sci.*, 2017, **490**, pp. 217–225

doi: 10.1049/mnl.2018.5049

[25] Lin H.L., Ye H.F., Xu B.Y., *ET AL.*: ' Ag_3PO_4 quantum dot sensitized $BiPO_4$: a novel P-N junction $Ag_3PO_4/BiPO_4$ with enhanced visible-light photocatalytic activity', *Catal. Commun.*, 2013, **37**, pp. 55–59
[26] Ratti M., Naddeo J.J., Tan Y.Y., *ET AL.*: 'Irradiation with visible light enhances the antibacterial toxicity of silver nanoparticles produced by laser ablation', *Appl. Phys. A-Mater. Sci. Process.*, 2016, **122**, pp. 1–7, doi: 10.1007/s00339-016-9935-8
[27] Liu L., Liu J.C., Sun D.D.: 'Graphene oxide enwrapped Ag_3PO_4 composite: towards a highly efficient and stable visible-light-induced photocatalyst for water purification', *Catal. Sci. Technol.*, 2012, **2**, pp. 2525–2532